Available online at www.sciencedirect.com
SCIENCE DIRECT®
Mechanics Research Communications 31 (2004) 677–688
MECHANICS RESEARCH COMMUNICATIONS
www.elsevier.com/locate/mechrescom

On the Fremond's constitutive model for shape memory alloys

Alessandro P. Baêta-Neves [a], Marcelo A. Savi [b], Pedro M.C.L. Pacheco [c,*]

[a] *Department of Mechanical and Materials Engineering, Instituto Militar de Engenharia, 22.290.270, Rio de Janeiro, Brazil*
[b] *COPPE—Department of Mechanical Engineering, Universidade Federal do Rio de Janeiro, 21.945.970, Cx. Postal 68.503, Rio de Janeiro, Brazil*
[c] *CEFET/RJ, Department of Mechanical Engineering, 20271.110, Rio de Janeiro, Brazil*

Available online 29 July 2004

Abstract

The remarkable properties of shape memory alloys have increasing the interest in applications in different areas varying from biomedical to aerospace hardware. Despite the large number of applications, the modeling of SMA is the objective of many researches developed in order to describe all details of its thermomechanical behavior. The present contribution revisits a constitutive model presented by Savi et al. (2002), which is built up on the classical Fremond's model, in order to contemplate the horizontal enlargement of the stress–strain hysteresis loop. Numerical simulations present qualitative agreement with experimental data, showing pseudoelastic, one-way and two-way shape memory effects.

Keywords: Shape memory alloys; Constitutive equations; Modeling and simulation

1. Introduction

Shape Memory Alloys (SMAs) are materials that present, among other characteristics, the capacity of undergoing large residual deformations, and then, after a temperature increase, recover its original shape. SMAs are easy to manufacture, relatively lightweight, and capable of producing high forces or displacements with low power consumption. They have also shown great potential as components of active composite materials or in association with another composites.

The mechanism behind SMAs remarkable behavior is related to martensitic phase transformation that the alloy undergoes when subjected to stress and/or temperature changes, which may be accomplished by

* Corresponding author. Tel./fax: +55 21 2569 4495.
E-mail addresses: savi@ufrj.br (M.A. Savi), calas@cefet-rj.br (P.M.C.L. Pacheco).

0093-6413/$ - see front matter
doi:10.1016/j.mechrescom.2004.06.007

electrically heating the SMA (Wayman, 1992). Detailed description of the shape memory effect and other phenomena associated with martensitic phase transformations, as well as examples of applications, may be found in different references (van Humbeeck, 1999; Duerig et al., 1999; Lagoudas et al., 1999; Shaw and Kyriakides, 1995; Rogers, 1995; Savi et al., 2002; Machado and Savi, 2003).

The thermomechanical behavior of shape memory alloys may be modeled either by microscopic or macroscopic point of view. Constitutive models consider phenomenological aspects of this behavior (Birman, 1997) and, despite the large number of applications, the modeling of SMA is the objective of many researches developed in order to describe all details of its thermomechanical behavior (James, 2000).

Savi et al. (2002) has presented a constitutive model in order to describe the thermomechanical behavior of SMAs. This model is based on Fremond's theory (Fremond, 1987, 1996) and includes four phases in the formulation: three variants of martensite and an austenitic phase. The inclusion of twinned martensite allows the description of a stable phase when the specimen is at a lower temperature and free of stress. Furthermore, different material parameters for austenitic and martensitic phases and new constraints are concerned. Thermal expansion and plastic strains are also included into the formulation. Hardening effect is represented by a combination of kinematics and isotropic behaviors. A plastic-phase transformation coupling is incorporated into the model allowing a correct description of the thermomechanical behavior of SMAs. Even though results predicted by the cited model present qualitative agreement with experiments, some improvements are necessary in order to obtain closer quantitative agreement. The present contribution revisits this formulation in order to contemplate the horizontal enlargement of the stress–strain hysteresis loop.

2. Constitutive model

Savi et al. (2002) proposes a constitutive model, which is built up on the contribution of Fremond (1987, 1996). Experimental tests related to SMAs shows that stress–strain hysteresis loop is larger in horizontal dimension than in the vertical one (Bo and Lagoudas, 1999; Sittner et al., 1995; Jackson et al., 1972). This evidence is usually related to a parameter called residual strain, ε_R, which is defined as the maximum value of the recoverable strain. In the original model, as well as the Fremond's model, the horizontal width of the stress–strain hysteresis loop is proportional to its vertical size and hence, it is difficult to fit experimental results. This motivates some alteration in the constitutive model in order to correct this discrepancy with experimental results, which is here discussed.

The modeling of SMA behavior is done within the scope of the standard generalized material (Lemaitre and Chaboche, 1990). With this assumption, the thermomechanical behavior can be described by the Helmholtz free energy, ψ, and the dual of the pseudo-potential of dissipation, ϕ^*. The thermodynamic state is completely defined by a finite number of state variables: deformation, ε, temperature, T, the volumetric fractions of martensitic variants, β_1 and β_2, which are associated with detwinned martensites (M+ and M−, respectively) and austenite (A), β_3. The fourth phase is associated with twinned martensite (M) and its volumetric fraction is β_4. The plastic phenomenon is described with the aid of plastic strain, ε^P, and the hardening effect is represented by a combination of kinematic and isotropic behaviors, described by variables μ and γ, respectively.

The expression of the Helmholtz free energy is proposed considering the free energy of each isolated phase, ψ_i. This procedure is adopted either in Fremond (1987, 1996) or in Savi et al. (2002), and here, terms related to the horizontal enlargement of the stress–strain hysteresis loop are also included into the formulation. After this definition, a free energy of the mixture can be written weighting each energy function with its volumetric fraction: $\rho\hat{\psi} = \sum_{i=1}^{4}\beta_i\psi_i + \widehat{\mathbf{J}}$, where $\widehat{\mathbf{J}}$ is the indicator function (Rockafellar, 1970; Lemaitre and Chaboche, 1990). Either $\hat{\psi}$ or $\widehat{\mathbf{J}}$ are functions of $\beta_i (i = 1, 2, 3, 4)$. As variable β_4 could be eliminated

since $\beta_1+\beta_2+\beta_3+\beta_4=1$, it is possible to rewrite the free energy of the mixture as a function of $\beta_i (i=1, 2, 3)$. After this, it is assumed an additive decomposition where the elastic strain, ε^{e}, may be written as: $\varepsilon^{\mathrm{e}}=\varepsilon-\varepsilon^{\mathrm{p}}-\alpha_{\mathrm{H}}(\beta_1-\beta_2)$. Parameter α_{H} is introduced in order to define the horizontal width of the stress–strain hysteresis loop. Therefore, the Helmholtz free energy has the following type

$$\rho\psi(\varepsilon,T,\beta_1,\beta_2,\beta_3,\varepsilon^{\mathrm{p}},\gamma,\mu)=\rho\tilde{\psi}(\varepsilon,T,\beta_1,\beta_2,\beta_3,\varepsilon^{\mathrm{p}},\gamma,\mu)+\mathbf{J}(\beta_1,\beta_2,\beta_3), \tag{1}$$

where ρ is the density and $\tilde{\psi}$ represents the differentiable part of the Helmholtz free energy, given by:

$$\begin{aligned}\rho\tilde{\psi}=&\beta_1\left[-\alpha(\varepsilon-\varepsilon^{\mathrm{p}})+\alpha\alpha_{\mathrm{H}}(\beta_1-\beta_2)-\frac{L_{\mathrm{M}}}{T_{\mathrm{M}}}(T-T_{\mathrm{M}})\right]\\&+\beta_2\left[\alpha(\varepsilon-\varepsilon^{\mathrm{p}})-\alpha\alpha_{\mathrm{H}}(\beta_1-\beta_2)-\frac{L_{\mathrm{M}}}{T_{\mathrm{M}}}(T-T_{\mathrm{M}})\right]\\&+\beta_3\left\{\frac{1}{2}(E_{\mathrm{A}}-E_{\mathrm{M}})[(\varepsilon-\varepsilon^{\mathrm{p}})-\alpha_{\mathrm{H}}(\beta_1-\beta_2)]^2-\frac{(L_{\mathrm{A}}+L_{\mathrm{M}})}{T_{\mathrm{M}}}(T-T_{\mathrm{M}})\right.\\&-(\Omega_{\mathrm{A}}-\Omega_{\mathrm{M}})(T-T_0)[(\varepsilon-\varepsilon^{\mathrm{p}})-\alpha_{\mathrm{H}}(\beta_1-\beta_2)]\\&\left.+\frac{1}{2}(K_{\mathrm{A}}-K_{\mathrm{M}})\gamma^2+\left(\frac{1}{2H_{\mathrm{A}}}-\frac{1}{2H_{\mathrm{M}}}\right)\mu^2\right\}+\frac{1}{2}E_{\mathrm{M}}[(\varepsilon-\varepsilon^{\mathrm{p}})-\alpha_{\mathrm{H}}(\beta_1-\beta_2)]^2\\&+\frac{L_{\mathrm{M}}}{T_{\mathrm{M}}}(T-T_{\mathrm{M}})-\Omega_{\mathrm{M}}(T-T_0)[(\varepsilon-\varepsilon^{\mathrm{p}})-\alpha_{\mathrm{H}}(\beta_1-\beta_2)]+\frac{1}{2}K_{\mathrm{M}}\gamma^2+\frac{1}{2H_{\mathrm{M}}}\mu^2.\end{aligned} \tag{2}$$

Here, α, $L_{\mathrm{M}}=L_{\mathrm{M}}(T)$ and $L_{\mathrm{A}}=L_{\mathrm{A}}(T)$ are material parameters that describe martensitic transformation, E_{M} and E_{A} represents the elastic moduli for martesitic and austenitic phases, respectively; Ω_{M} and Ω_{A} represents the thermal expansion coefficient for martensitic and austenitic phases, respectively; K_{M} and K_{A} are the plastic moduli for martensitic and austenitic phases while H_{M} and H_{A} are the kinematic hardening moduli for martensitic and austenitic phases; T_{M} is a temperature below which the martensitic phase starts its formation in the absence of stress while T_0 is a reference temperature.

The indicator function $\mathbf{J}$ (Rockafellar, 1970; Lemaitre and Chaboche, 1990) is related to the tetrahedron π of the set (Fig. 1)

$$\pi=\left\{\beta_i\in\Re\left|\begin{array}{l}0\leqslant\beta_i\leqslant 1(i=1,2,3);\beta_1+\beta_2+\beta_3\leqslant 1;\\ \beta_1=\beta_2=0 \text{ if } \sigma=0 \text{ and } \beta_1^S=\beta_2^S=0\end{array}\right.\right\}. \tag{3}$$

This set also contemplates the constraints where detwinned martensites, M+ and M−, are induced by stress fields. The definition of this physical aspect is considered when $\sigma=0$, and $\beta_1^S=\beta_2^S=0$, where β_1^S and β_2^S are the values of β_1 and β_2, respectively, when the phase transformation begins to take place.

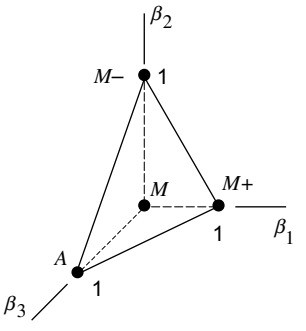

Fig. 1. Tetrahedron of the constraints π.

With these assumptions, state equations can be obtained from the Helmholtz free energy as follows (Lemaitre and Chaboche, 1990):

$$\sigma = \rho\frac{\partial\psi}{\partial\varepsilon} = E(\varepsilon-\varepsilon^{\mathrm{p}}) + (\alpha + E\alpha_{\mathrm{H}})(\beta_2-\beta_1) - \Omega(T-T_0), \tag{4}$$

$$\begin{aligned} B_1 \in -\rho\frac{\partial\psi}{\partial B_1} \\ = \alpha(\varepsilon-\varepsilon^{\mathrm{p}}) + \frac{L_{\mathrm{M}}}{T_{\mathrm{M}}}(T-T_{\mathrm{M}}) + \alpha_{\mathrm{H}}[E(\varepsilon-\varepsilon^{\mathrm{p}}) + (2\alpha+E\alpha_{\mathrm{H}})(\beta_2-\beta_1) - \Omega(T-T_0)] - \partial_1 J, \end{aligned} \tag{5}$$

$$\begin{aligned} B_2 \in -\rho\frac{\partial\psi}{\partial B_2} \\ = \alpha(\varepsilon-\varepsilon^{\mathrm{p}}) + \frac{L_{\mathrm{M}}}{T_{\mathrm{M}}}(T-T_{\mathrm{M}}) + \alpha_{\mathrm{H}}[E(\varepsilon-\varepsilon^{\mathrm{p}}) + (2\alpha+E\alpha_{\mathrm{H}})(\beta_2-\beta_1) - \Omega(T-T_0)] - \partial_2 J, \end{aligned} \tag{6}$$

$$\begin{aligned} B_3 \in -\rho\frac{\partial\psi}{\partial B_3} \\ = -\frac{1}{2}(E_{\mathrm{A}}-E_{\mathrm{M}})[(\varepsilon-\varepsilon^{\mathrm{p}}) - \alpha_{\mathrm{H}}(\beta_1-\beta_2)]^2 + \frac{L_{\mathrm{M}}+L_{\mathrm{A}}}{T_{\mathrm{M}}}(T-T_{\mathrm{M}}) + (\Omega_{\mathrm{A}}-\Omega_{\mathrm{M}})(T-T_0)[(\varepsilon-\varepsilon^{\mathrm{p}}) \\ - \alpha_{\mathrm{H}}(\beta_1-\beta_2)] - \frac{1}{2}(K_{\mathrm{A}}-K_{\mathrm{M}})\gamma^2 - \left(\frac{1}{2H_{\mathrm{A}}} - \frac{1}{2H_{\mathrm{M}}}\right)\mu^2 - \partial_3 J, \end{aligned} \tag{7}$$

$$X = -\rho\frac{\partial\psi}{\partial\varepsilon^{\mathrm{p}}} = E(\varepsilon-\varepsilon^{\mathrm{p}}) + (\alpha+E\alpha_{\mathrm{H}})(\beta_2-\beta_1) - \Omega(T-T_0) = \sigma, \tag{8}$$

$$Y = -\rho\frac{\partial\psi}{\partial\gamma} = -K\gamma, \tag{9}$$

$$Z = -\rho\frac{\partial\psi}{\partial\mu} = -\frac{1}{H}\mu, \tag{10}$$

where B_i are thermodynamic forces related to SMA behavior, while X, Y and Z are associated with plastic behavior; σ represents the uniaxial stress; ∂_i is the *sub-differential* with respect to β_i (Rockafellar, 1970). Lagrange multipliers offer a good alternative to represent sub-differentials of the indicator function (Savi and Braga, 1993). Notice that the following definitions are considered in the previous equations

$$E = E_{\mathrm{M}} - \beta_3(E_{\mathrm{M}}-E_{\mathrm{A}}), \tag{11}$$

$$\Omega = \Omega_{\mathrm{M}} - \beta_3(\Omega_{\mathrm{M}}-\Omega_{\mathrm{A}}), \tag{12}$$

$$K = K_{\mathrm{M}} - \beta_3(K_{\mathrm{M}}-K_{\mathrm{A}}), \tag{13}$$

$$\frac{1}{H} = \frac{1}{H_{\mathrm{M}}} - \beta_3\left(\frac{1}{H_{\mathrm{M}}} - \frac{1}{H_{\mathrm{A}}}\right). \tag{14}$$

The dual of the pseudo-potential of dissipation is similar to the one proposed by Savi et al. (2002), and has the following type

$$\phi^* = \frac{1}{2\eta}\left[(B_1+\eta_{\mathrm{ci}}Y+\eta_{\mathrm{ck}}Z)^2 + (B_2+\eta_{\mathrm{ci}}Y+\eta_{\mathrm{ck}}Z)^2 + (B_3+\eta_{\mathrm{ci}}Y+\eta_{\mathrm{ck}}Z)^2\right] + I_f, \tag{15}$$

where I_f is the indicator function related to the yield surface defined as follows (Lemaitre and Chaboche, 1990):

$$f(X,Y,Z) = |X + HZ| - (\sigma_Y - Y) \quad \text{or} \quad f(\sigma,\mu,\gamma) = |\sigma - \mu| - (\sigma_Y - K\gamma). \tag{16}$$

Parameter η is associated with the internal dissipation of the material while η_{ci} and η_{ck} are related to plastic-phase transformation coupling. The parameter η_{ci} is associated with isotropic hardening coupling while η_{ck} is associated with kinematic hardening coupling. At this point, it is possible to write the following complementary equations (Lemaitre and Chaboche, 1990; Savi et al., 2002):

$$\dot{\beta}_1 \in \partial_{B_1}\phi^* = \frac{B_1}{\eta} + \frac{\eta_{ci}}{\eta}Y + \frac{\eta_{ck}}{\eta}Z = \frac{B_1}{\eta} - \frac{\eta_{ci}}{\eta}K\gamma - \frac{\eta_{ck}}{\eta}\frac{\mu}{H}, \tag{17}$$

$$\dot{\beta}_2 \in \partial_{B_2}\phi^* = \frac{B_2}{\eta} + \frac{\eta_{ci}}{\eta}Y + \frac{\eta_{ck}}{\eta}Z = \frac{B_2}{\eta} - \frac{\eta_{ci}}{\eta}K\gamma - \frac{\eta_{ck}}{\eta}\frac{\mu}{H}, \tag{18}$$

$$\dot{\beta}_3 \in \partial_{B_3}\phi^* = \frac{B_3}{\eta} - \frac{\eta_{ci}}{\eta}Y - \frac{\eta_{ck}}{\eta}Z = \frac{B_3}{\eta} - \frac{\eta_{ci}}{\eta}K\gamma + \frac{\eta_{ck}}{\eta}\frac{\mu}{H}, \tag{19}$$

$$\dot{\varepsilon}^p \in \partial_X\phi^* = \lambda \operatorname{sign}(X + HZ) = \lambda \operatorname{sign}(\sigma - \mu), \tag{20}$$

$$\dot{\gamma} \in \partial_Y\phi^* = \lambda + \eta_{ci}(\dot{\beta}_1 + \dot{\beta}_2 - \dot{\beta}_3) = |\dot{\varepsilon}^p| + \eta_{ci}(\dot{\beta}_1 + \dot{\beta}_2 - \dot{\beta}_3), \tag{21}$$

$$\dot{\mu} \in \partial_Z\phi^* = \lambda H \operatorname{sign}(X + HZ) + \eta_{ck}(\dot{\beta}_1 + \dot{\beta}_2 - \dot{\beta}_3) = H\dot{\varepsilon}^p + \eta_{ck}(\dot{\beta}_1 + \dot{\beta}_2 - \dot{\beta}_3), \tag{22}$$

where λ is the classical plastic multiplier. The irreversible nature of plastic flow is represented by means of the *Kuhn–Tucker conditions*. Another constraint must be satisfied when $f(\sigma,\gamma,\mu) = 0$. It is referred as *consistency condition* and corresponds to the physical requirement that a stress point on the yield surface must persist on it. These conditions are presented as follows (Simo and Hughes, 1998):

$$\lambda \geqslant 0;\ f(\sigma,\gamma,\mu) \leqslant 0;\ \lambda f(\sigma,\gamma,\mu) = 0;\ \lambda \dot{f}(\sigma,\gamma,\mu) = 0 \quad \text{if } f(\sigma,\gamma,\mu) = 0 \tag{23}$$

These equations form a complete set of constitutive equations. Since the pseudo-potential of dissipation is convex, positive and vanishes at the origin, the Clausius–Duhen inequality (Eringen, 1967), is automatically satisfied if the entropy is defined as $s = -\partial_\psi/\partial_T$.

Moreover, it is important to consider the definition of the parameters $L_M = L_M(T)$ and $L_A = L_A(T)$, which are obtained assuming $\dot{\beta}_1 = 0$ and $\varepsilon = \varepsilon_R$ in a critical temperature, T_C, below which there is no change in stress–strain hysteresis loop position. With this aim, it is necessary to define

$$T_C = T_M\left[\frac{L_M E_M + \alpha(\Omega_M T_0 - \alpha)}{L_M E_M + \alpha\Omega_M T_M}\right], \tag{24}$$

$$\alpha_H = \varepsilon_R + \frac{L_M}{\alpha T_M}(T_C - T_M). \tag{25}$$

Hence, one wishes to limit the displacement of the hysteresis loop with respect to temperature when $T < T_C$. With this aim, the term $L_M(T)$ is defined in such a way that $\frac{L_M(T)}{T_M}(T - T_M)$ becomes a constant for $T < T_C$. Also, $L_M(T) + L_A(T) = 2L$, and therefore, the following expressions are obtained

$$L_M(T) = \begin{cases} L_M = L, & \text{if } T \geqslant T_C \\ L_M = L\frac{(T_C - T_M)}{(T - T_M)}, & \text{if } T < T_C, \end{cases} \tag{26}$$

$$L_{\mathrm{A}}(T) = \begin{cases} L_{\mathrm{A}} = L, & \text{if } T \geqslant T_{\mathrm{C}} \\ L_{\mathrm{A}} = 2L - \left[L\frac{(T_{\mathrm{C}} - T_{\mathrm{M}})}{(T - T_{\mathrm{M}})}\right], & \text{if } T < T_{\mathrm{C}}. \end{cases} \tag{27}$$

A comparison between this new model and the original one (Savi et al., 2002) shows that this new set of constitutive equations promote the horizontal enlargement of the stress–strain hysteresis loop. Phase transformations due to thermal loads, free of stress (A → M or M → A), are not altered with the discussed modifications. Therefore, these modifications are concerned with pseudoelastic and shape memory effects.

With respect to numerical procedure, a similar iterative procedure based on the operator split technique (Ortiz et al., 1983), the orthogonal projection algorithm (Savi and Braga, 1993) and the return mapping algorithm (Simo and Taylor, 1986; Simo and Hughes, 1998) is employed.

3. Material parameters

The response predicted by the proposed model is evaluated considering a SMA specimen with typical properties of a Ni–Ti alloy (Table 1), subjected to different thermomechanical loadings. Stress-driving or temperature-driving simulations are carried out. This section presents a brief discussion of material parameters, showing the influence of the proposed modifications in the original model.

The yield limit σ_{Y} has a linear variation with T evaluated with the following expression:

$$T \leqslant T_{\mathrm{M}} \Rightarrow \sigma_{\mathrm{Y}} = \sigma_{\mathrm{Y}}^{\mathrm{M}}, \tag{28}$$

$$T_{\mathrm{M}} < T \leqslant T_{\mathrm{A}} \Rightarrow \sigma_{\mathrm{Y}} = \frac{\sigma_{\mathrm{Y}}^{\mathrm{M}}(T_{\mathrm{A}} - T) + \sigma_{\mathrm{Y}}^{\mathrm{A},i}(T - T_{\mathrm{M}})}{T_{\mathrm{A}} - T_{\mathrm{M}}}, \tag{29}$$

$$T_{\mathrm{A}} < T \leqslant T_{F} \Rightarrow \sigma_{\mathrm{Y}} = \frac{\sigma_{\mathrm{Y}}^{\mathrm{A},i}(T_{\mathrm{F}} - T) + \sigma_{\mathrm{Y}}^{\mathrm{A},i}(T - T_{\mathrm{A}})}{T_{\mathrm{F}} - T_{\mathrm{A}}}, \tag{30}$$

where T_{F} is used to determine the angular coefficient of the linear interpolation. Moreover, one considers $\varepsilon_{\mathrm{R}} = 6.7\%$ (Brinson, 1993).

In order to observe the difference between the proposed model and the original one, a pseudoelastic simulation is considered. Three different situations are treated. For the original model, $\alpha_{\mathrm{H}} = 0$ and the following parameters are calculated (Savi et al., 2002): $\varepsilon_{\mathrm{R}} = 0.0033$, $T_{\mathrm{C}} = 282.04$ K and $L = 9.18$ MPa/K. On the other hand, the new model considers the introduction of parameter α_{H}, which may be calculated from the value of the maximum residual strain ε_R (Eqs. (24) and (25)). Hence, two different situations are analyzed. At first consider, $L = 9.18$ MPa (similar to the previous example, related to the original model), and therefore, $T_{\mathrm{C}} = 282.04$ K (9.04 °C) and $\alpha_{\mathrm{H}} = 0.0637$. Another situation considers $L = 212$ MPa, and hence,

Table 1
Thermomechanial properties

E_{A} (GPa)	E_{M} (GPa)	α (MPa)	η (MPa/K)		
67	26.30	89.42	0.07		
T_{M} (K)	T_{A} (K)	T_0 (K)	Ω_{A} (MPa/K)	Ω_{M} (MPa/K)	Ω_Y^{M} (MPa)
291.40	307.50	298	0.74	0.17	70
$\sigma_{\mathrm{Y}}^{\mathrm{A},i}$ (MPa)	$\sigma_{\mathrm{Y}}^{\mathrm{A},f}$ (MPa)	K_{A} (GPa)	K_{M} (GPa)	H_{A} (GPa)	H_{M} (GPa)
690	257.72	1.40	0.40	0.40	0.11

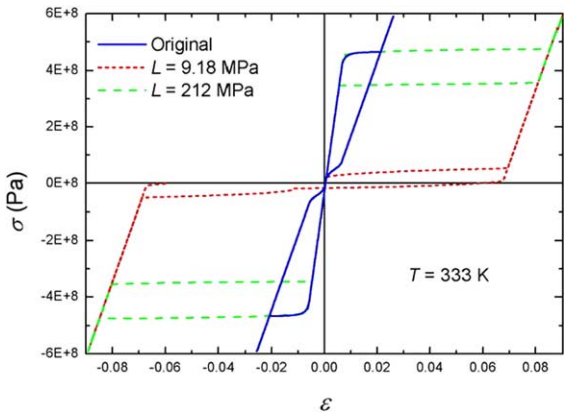

Fig. 2. Stress–strain curve related to pseudoelastic effect for different parameters L.

$T_C = 290.99$ K (17.99 °C) and $\alpha_H = 0.0637$. Fig. 2 shows three different curves related to these situations. Notice the difference on the horizontal width of the stress–strain hysteresis loop and also the alteration of the vertical position as parameter L is modified.

It should be pointed out that the new model has different characteristics to phase transformation velocity. During transformation A → M+, phase transformation is slower as β_3 grow. On the other hand, during transformation M+ → A, the transformation is faster. In order to control this process of phase transformation it is possible to consider different values to the parameter η, which is related to internal dissipation, for loading and unloading process. Therefore,

$$\begin{cases} \eta = \eta_L & \text{if } |\dot{\varepsilon}| > 0 \\ \eta = \eta_U & \text{if } |\dot{\varepsilon}| < 0 \end{cases}, \tag{31}$$

where η_L and η_U are internal dissipation parameters related to load and unload process, respectively.

4. Numerical simulations

In this section, numerical simulations related to pseudoelastic and shape memory effect are considered in order to evaluate the general behavior of the proposed model. Parameters presented in Table 1 and also the modifications proposed in the previous section are considered, that is: $\eta_L = 0.07$ MPa s and $\eta_U = 0.1225$ MPa s.

At first, pseudoelastic effect is concerned regarding a SMA specimen subjected to an isothermal mechanical loading performed at $T = 333$ K ($T > T_A$). The stress–strain curve for stress-driving case is presented in Fig. 3a. Fig. 3b shows the volumetric fraction evolution of each phase. When the specimen is free of stress, the austenitic phase is stable. After this, positive stresses induce the formation of the M+ variant of martensite. The unloading process induces the austenite formation again. When there are negative stresses, the M− variant of martensite is induced. Finally, the unloading process induces the formation of the austenitic phase (A). Finished the loading–unloading process the specimen presents no residual strain.

At this point, it is considered that the load process reaches the plastic region of the material. Assuming, $\eta_{ci} = \eta_{ck} = 0.02$, the stress–strain curve is shown in Fig. 4. As expected, the plastification process introduces residual strain that cannot be eliminated by the reverse phase transformation.

Shape memory effect is now focused regarding a thermomechanical load depicted in Fig. 5. Firstly, a constant temperature $T = 263$ K ($T < T_M$) is considered, where the martensitic phase is stable. After

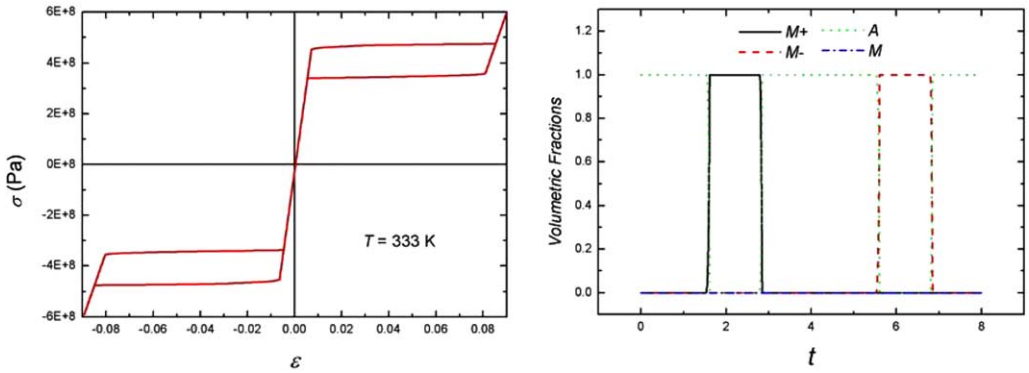

Fig. 3. Pseudoelastic effect.

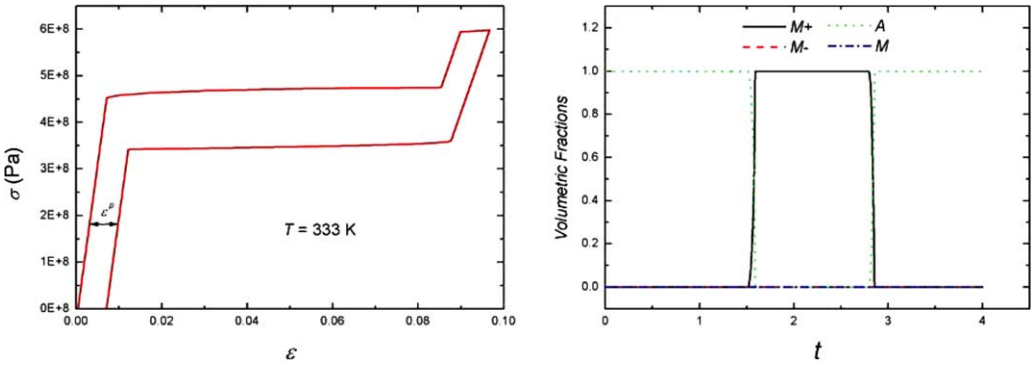

Fig. 4. Pseudoelastic effect with plastic strains.

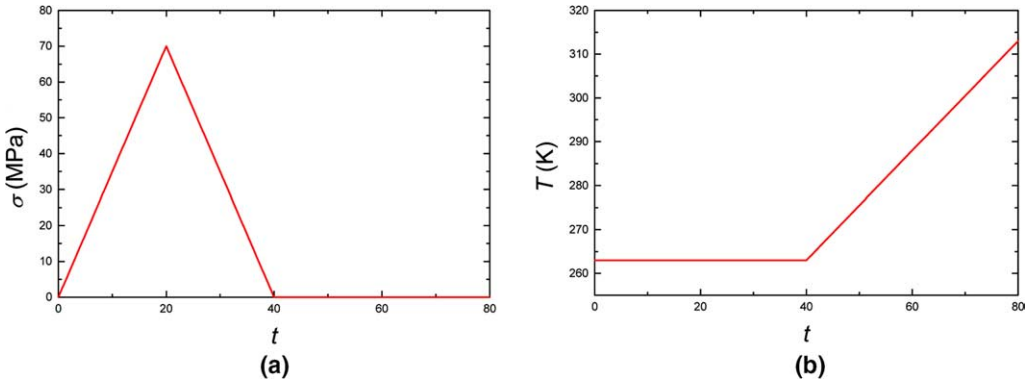

Fig. 5. Thermomechanical load process. (a) Stress and (b) temperature.

mechanical loading–unloading process, the specimen presents a residual strain that can be eliminated by a subsequent thermal loading (Fig. 6). The heating process induces the transformation from detwinned martensite, M+, to twinned martensite, M and, for higher temperatures, the austenitic phase (A). Fig. 6b shows

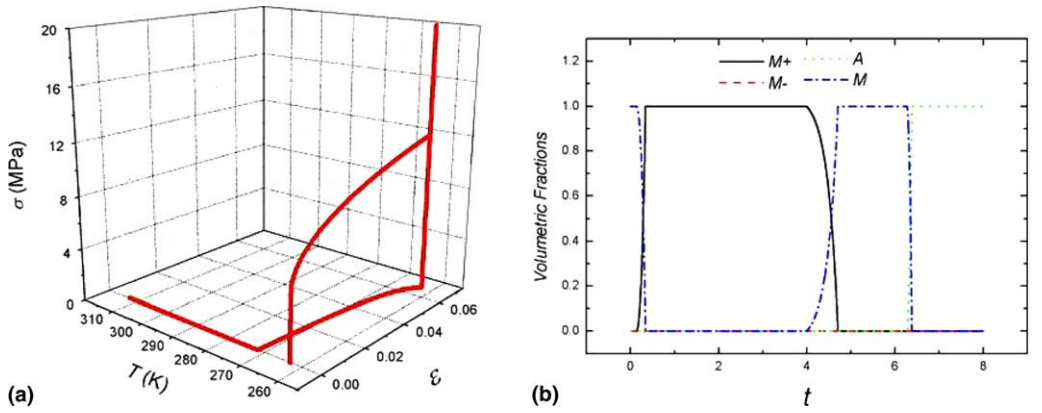

Fig. 6. Shape memory effect.

the volumetric fraction evolution of each phase, pointing out the cited phase transformation. Notice that the large amount of residual strain is a consequence of the enlargement of the horizontal width of the hysteresis loop.

Considering a loading–unloading process similar to the previous simulation that reaches the plastic region of the material, and assuming, $\eta_{ci} = \eta_{ck} = 0.02$, the stress–strain curve is shown in Fig. 7. The horizontal line represents the material yield limit for 263 K. As expected, the plastification process introduces residual strain that cannot be eliminated by the reverse phase transformation, promoted by the thermal load.

Two-way shape memory effect is now considered (Bo and Lagoudas, 1999; Zhang et al., 1991). With this aim, stress-induced martensite training (SIM training), represented in Fig. 8, is simulated. Initially, five cycles of an isothermal mechanical process ($T = 333$ K), with increasing maximum values, is considered. Each cycle causes plastic strains. Finishing this mechanical process, thermal load is applied with a constant value of mechanical load ($\sigma = 50$ MPa).

Plasticity and phase transformation are coupled by the parameter $\eta_{ci} = \eta_{ck} = 0.05$. Fig. 9 shows the stress–strain curve during SIM training. Notice the growth of plastic strains during each load cycle. Finished this process, SMA presents phase transformation A → M+ during cooling and M+ → A during heating. This behavior is related to the two-way shape memory effect that allows one to associate each phase to

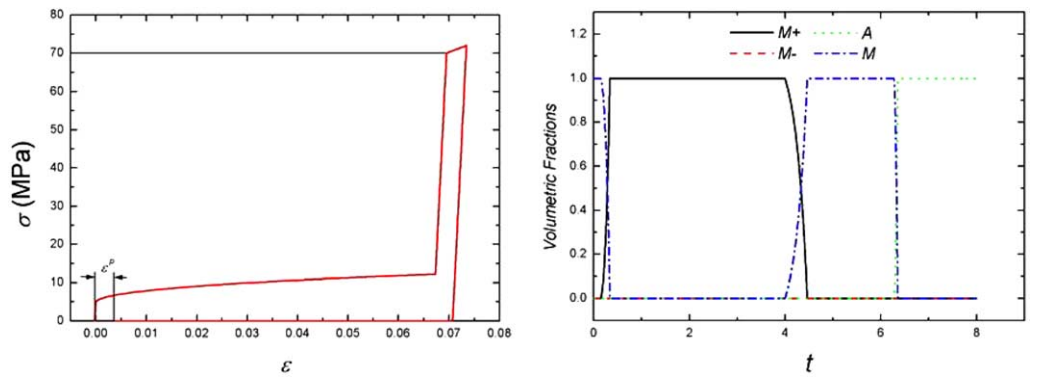

Fig. 7. Shape memory effect with plastic strains.

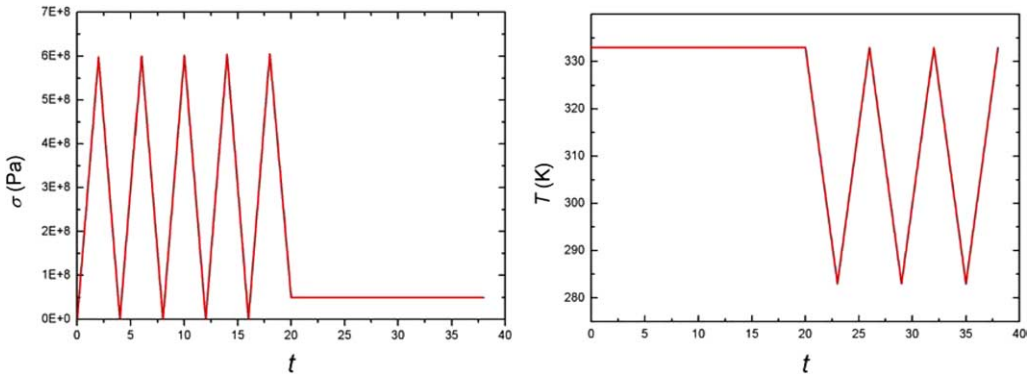

Fig. 8. Thermomechanical load process associated with two-way shape memory effect (SIM training).

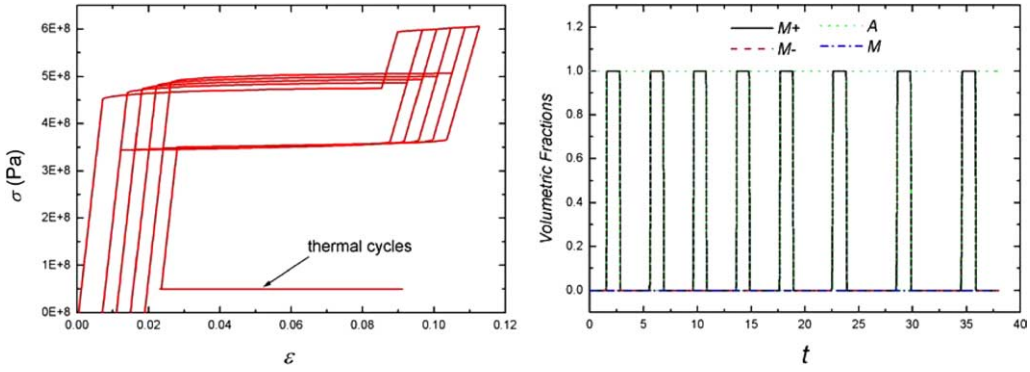

Fig. 9. Two-way shape memory effect (SIM training).

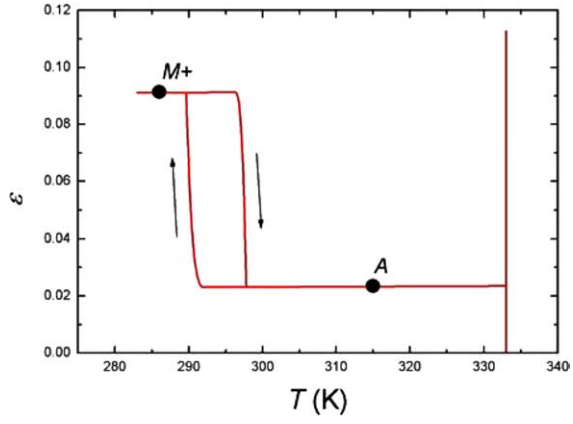

Fig. 10. Two-way shape memory effect.

a different form. Fig. 10 shows a strain-temperature curve, representing this effect. It should be pointed out that the description of this phenomenon is related to the plastic-phase transformation coupling introduced in the proposed model.

5. Conclusions

This contribution concerns with the modeling and simulation of shape memory alloys. A constitutive model proposed by Savi et al. (2002) that is built up on the contribution of Fremond (1987, 1996), is analyzed in order to improve predicted results to be closer to experimental data. This model includes four phases into the formulation, and different material parameters for austenitic and martensitic phases. Thermal expansion and plastic strains are also included into the formulation. Hardening effect is represented by a combination of kinematic and isotropic behaviors and a plastic-phase transformation coupling is considered. The present contribution alters the original model in order to contemplate the horizontal enlargement of the stress–strain hysteresis loop. Numerical results show that the proposed model is capable to capture the general behavior of experimental data. Pseudoelastic, one-way and two-way shape memory effects have proper description with the presented model. Nevertheless, there are features that still needed to be contemplated in the proposed model. The elimination of the softening behavior for strain driving case and the correct description of internal loops observed during cyclic loads associated with incomplete phase transformations are some examples.

Acknowledgments

The authors acknowledge the support of the Brazilian Agencies CNPq and CAPES.

References

Birman, V., 1997. Review of mechanics of shape memory alloy structures. Applied Mechanics Review 50, 629–645.

Bo, Z.H., Lagoudas, D.C., 1999. Thermomechanical modeling of polycrystalline SMAs under cyclic loading, part III: evolution of plastic strains and two-way shape memory effect. International Journal of Engineering Science 37, 1175–1203.

Brinson, L.C., 1993. One dimensional constitutive behavior of shape memory alloys: thermomechanical derivation with non-constant material functions and redefined martensite internal variable. Journal of Intelligent Material Systems and Structures 4, 229–242.

Duerig, T., Pelton, A., Stöckel, D., 1999. An overview of nitinol medical applications. Materials Science and Engineering A 273–275, 149–160.

Eringen, A.C., 1967. Mechanics of Continua. John Wiley & Sons.

Fremond, M., 1987. Matériaux à Mémoire de Forme, C.R. Acad. Sci. Paris, Tome 34, s.II, n.7, pp. 239–244.

Fremond, M., 1996. Shape Memory Alloy: A Thermomechanical Macroscopic Theory, CISM Courses and Lectures. Springer-Verlag.

Jackson, C.M., Wagner, H.J., Wasilewski, R.J., 1972. 55-Nitinol—the alloy with a memory: its physical metallurgy, properties, and applications. NASA-SP-5110.

James, R.D., 2000. New materials from theory: trends in the development of active materials. International Journal of Solids and Structures 37, 239–250.

Lagoudas, D.C., Rediniotis, O.K., Khan, M.M., 1999. Applications of shape memory alloys to bioengineering and biomedical technology. In: Proceeding of the Fourth International Workshop on Mathematical Methods in Scattering Theory and Biomedical Technology, October 1999, Perdika, Greece.

Lemaitre, J., Chaboche, J.-L., 1990. Mechanics of Solid Materials. Cambridge University Press.

Machado, L.G., Savi, M.A., 2003. Medical applications of shape memory alloys. Brazilian Journal of Medical and Biological Research 36 (6), 683–691.

Ortiz, M., Pinsky, P.M., Taylor, R.L., 1983. Operator split methods for the numerical solution of the elastoplastic dynamic problem. Computer Methods of Applied Mechanics and Engineering 39, 137–157.

Rockafellar, R.T., 1970. Convex Analysis. Princeton Press.

Rogers, C.A., 1995. Intelligent materials. Scientific American (September), 122–127.

Savi, M.A., Paiva, A., Baêta-Neves, A.P., Pacheco, P.M.C.L., 2002. Phenomenological modeling and numerical simulation of shape memory alloys: a thermo-plastic-phase transformation coupled model. Journal of Intelligent Materials Systems and Structures 3 (5), 261–273.

Savi, M.A., Braga, A.M.B., 1993. Chaotic vibrations of an oscillator with shape memory. Journal of the Brazilian Society for Mechanical Sciences 15 (1), 1–20.

Shaw, J.A., Kyriakides, S., 1995. Thermomechanical aspects of NiTi. Journal of Mechanics Physics Solids 43, 243–1281.

Simo, J.C., Hughes, T.J.R., 1998. Computational Inelasticity. Springer.

Simo, J.C., Taylor, R.L., 1986. A return mapping algorithm for plane stress elastoplasticity. International Journal for Numerical Methods in Engineering 22, 649–670.

Sittner, P., Hara, Y., Tokuda, M., 1995. Experimental study on the thermoelastic martensitic transformation in shape memory alloy polycrystal induced by combined external forces. Metallurgical and Materials Transactions A 26, 2923–2935.

van Humbeeck, J., 1999. Non-medical applications of shape memory alloys. Materials Science and Engineering A 273–275, 134–148.

Wayman, C.M., 1992. Thermoelastic martensitic transformations and the nature of the shape memory effect. In: Proceedings of the International Conference on Martensitic Transformations—ICOMAT-92, 20–24 July 1992, Monterey, California, USA.

Zhang, X.D., Rogers, C.A., Liang, C., 1991. Modeling of two-way shape memory effect. ASME—Smart Structures and Materials 24, 79–90.